Available online at www.sciencedirect.com

ScienceDirect

Mendeleev Commun., 2022, **32**, 311–314

Mendeleev Communications

Solvate phases crystallizing from hybrid halide perovskite solutions: chemical classification and structural relations

Andrey A. Petrov,[a] Ekaterina I. Marchenko,[a,b] Sergey A. Fateev,[a] Li Yumao,[a,c] Eugene A. Goodilin[a,d] and Alexey B. Tarasov*[a]

[a] *Department of Materials Science, M. V. Lomonosov Moscow State University, 119991 Moscow, Russian Federation. E-mail: alexey.bor.tarasov@yandex.ru*
[b] *Department of Geology, M. V. Lomonosov Moscow State University, 119991 Moscow, Russian Federation*
[c] *Faculty of Materials Science, Shenzhen MSU-BIT University, Longgang District, 517182 Shenzhen, China*
[d] *Department of Chemistry, M. V. Lomonosov Moscow State University, 119991 Moscow, Russian Federation*

DOI: 10.1016/j.mencom.2022.05.006

Solution crystallization techniques of hybrid lead halides for perovskite photovoltaics, while remaining the most common method for fabricating solar cells, are inevitably complicated by the formation of numerous intermediate solvates that predetermine the morphology and properties of the final perovskite light-harvesting layer. Here, for the first time, a chemical classification of known solvates is proposed based on a comprehensive analysis of their structural features and relationships with possible structural types.

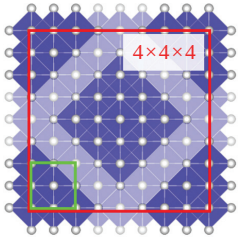

Keywords: hybrid perovskites, hybrid halide perovskites, adducts, solvates, intermediate phases, DMF, DMSO, GBL.

Hybrid organic–inorganic perovskites of the general formula ABX_3 [A = $MeNH_3^+$ (MA), $CH(NH_2)_2^+$ (FA); B = Pb^{2+}, Sn^{2+}; X = I^-, Br^-] demonstrate a combination of outstanding properties such as high absorption coefficients, high charge carrier mobility and intense luminescence, and thus represent a promising new class of materials for solar cells and optoelectronics.[1–4] One of the most attractive properties of such materials is their solubility in common solvents with high donor numbers and dipole moment, such as dimethyl sulfoxide (DMSO), *N*,*N*-dimethylformamide (DMF) and γ-butyrolactone (GBL).[5–7] However, such high solubility, being a key factor in the successful solution processing of perovskite photovoltaic devices, is paid for by the intense interaction of these solvents with perovskite constituents.[6] This, in turn, causes the formation of many intermediate solvate phases, which entails difficulties in controlling the reproducibility of morphology and properties.[8]

Sang Il Seok *et al.* pointed out the crucial role of intermediate phases in the formation of perovskite films and their morphology.[9] In 2014, an unknown intermediate phase [$(MA)_2Pb_3I_8{\cdot}2DMSO$, as we know it today] was observed upon crystallization of a $MAPb(I_{2.9}Br_{0.1})_3$ solution in a GBL/DMSO mixture after dripping toluene as an antisolvent. A year later, Nam-Gyu Park *et al.* proposed a Lewis base adduct approach for the fabrication of high-efficiency solar cells, also emphasizing the strong interaction with DMSO as a key point for the formation of smooth uniform $MAPbI_3$ films.[10] Later, it was shown that the intermediate phases act as structure-directing agents controlling the morphology of the final perovskite phase formed upon their decomposition.[11]

Direct studies of the crystallization process of hybrid perovskites further confirmed the crucial role of the intermediate phases in the properties of final materials. Besides, these studies revealed many haloplumbate solvate phases with methylammonium and formamidinium cations. In particular, it was found that crystallization of $MAPbI_3$ from DMF and DMSO solutions can give intermediate phases such as $(MA)_2Pb_3I_8{\cdot}2Solv$, $(MA)_3PbI_5{\cdot}Solv$ (Solv = DMF or DMSO) and $(MA)_2Pb_2I_6{\cdot}2DMF$, depending on the ratio of precursors.[12] More recently, the structures of four new phases of DMF and DMSO solvates of haloplumbates with formamidinium cations have also been reported.[13] In addition, it was shown that there are also GBL solvates of haloplumbates, which deteriorate the morphology and produce compositional inhomogeneity upon their decomposition in target perovskite films.[8]

Another important application of solvate phases is their direct use as convenient precursors. For instance, the $PbI_2{\cdot}DMSO$ adduct was proposed as a precursor in the intramolecular exchange reaction:[14]

$$PbI_2{\cdot}DMSO + FAI/MABr \rightarrow (FA/MA)Pb(I/Br)_3 + DMSO.$$

Using this approach, perovskite solar cells with certified power conversion efficiency as high as 23.9% have recently been fabricated.[15] A similar intramolecular exchange strategy for fabricating a perovskite film has also been applied using an 1-methyl-2-pyrrolidone (NMP) adduct (presumably $PbI_2{\cdot}NMP$) as a precursor.[16] In addition, hybrid halometallates can be considered as chemosensors due to their reversible solvation and its effect on their optical properties.[17,18]

The rapid growth in the number of detected haloplumbate solvates necessitates their comparative crystal chemical analysis and classification. Although there are several studies on the structure–property relationships of halometallates and their crystallographic diversity,[19–22] in this study we focus on haloplumbates relevant to the synthesis of hybrid halide perovskites in order to reveal their proximity to PbI_2 or $MAPbI_3$ structures

Table 1 Known solvate haloplumbate phases.[a]

Organic cation	Solvent	Adduct stoichiometry		
		PbX_2-excessive	Stoichiometric	PbX_2-deficient
MA^+	DMSO	$(MA)_2Pb_3I_8·2DMSO$[23,24]	–	$(MA)_3PbI_5·DMSO$[23]
	DMF	$(MA)_2Pb_3I_8·2DMF$[12]	$MAPbI_3·DMF$[12,25,26] $MAPbBr_3·DMF$[27]	$(MA)_3PbI_5·DMF$[12]
	GBL	$(MA)_2Pb_3I_8·2GBL$[8] $(MA)_8[Pb_{18}I_{44}]·x\,GBL$[8] $(MA)_{8-z}Pb_{18-\delta/2}I_{44-\delta-z}·y\,GBL$[8]	–	–
FA^+	DMSO	–	$FAPbBr_3·DMSO$[28]	$(FA)_5Pb_2I_9·0.5DMSO$[13] $(FA)_2PbBr_4·DMSO$[13]
	DMF	$(FA)_2Pb_3I_8·4DMF$[13]	$FAPbI_3·2DMF$[13,29]	–
	GBL	$(FA)_8[Pb_{18}I_{44}]·x\,GBL$[8]	–	–
No	DMSO	$PbI_2·DMSO$[23] $PbI_2·2DMSO$[23] $PbBr_2·2DMSO$[30]		
	DMF	$PbI_2·DMF$[23,31] $PbBr_2·DMF$[32]		
	GBL	–		

[a] A long dash means that the corresponding phases do not exist or have not yet been identified.

and, therefore, to better understand the mechanisms of their transformation into perovskite phases.

In this study, we propose the first classification of haloplumbate solvates with DMF, DMSO and GBL known to date and based on their chemical composition. Furthermore, we provide a detailed crystal chemical analysis of all haloplumbate solvates known so far when considering the similarity of structural motifs with respect to NaCl and NiAs structure types.

To the best of our knowledge, 20 reported solvate phases of haloplumbates with DMF, DMSO and GBL are known (Table 1). Based on the composition of the solvates, we propose to divide them into three main groups: (1) solvates containing MA^+ cations, (2) solvates containing FA^+ cations and (3) solvates without organic cations. From a practical point of view, it is reasonable to divide each of these groups into the following three subgroups: (1) PbX_2-excessive, (2) stoichiometric and (3) PbX_2-deficient. Stoichiometric solvates decompose directly to perovskite, PbX_2-deficient phases can also be easily converted to perovskite by annealing to remove the excess of organic halide. The formation of PbX_2-excessive phases is the most undesirable case, unless they quickly precipitate to form small crystals together with organic halides, which subsequently react with them, as is observed in the case of an antisolvent approach.[23]

For further analysis of the crystal structures of the solvate phases and to establish their similarity with the structures of perovskite and PbI_2, we considered the structures of the solvates taking into account close-packed layers and connectivity features of the PbX_6 octahedra.

Many common crystals have a structure described by cubic or hexagonal close-packed sphere packing, realized in NaCl or NiAs structure types, respectively. In these structures, close-packed layers are formed by anions, while octahedral voids are filled with cations. In particular, perovskite and PbI_2 (CdI_2 structure type) can be considered as subtraction phases belonging to the NiAs and NaCl structure types, respectively. The solvate structures from Table 1 can be divided into three general groups: (1) structures with corner-sharing octahedra closely related to the NaCl structure type, (2) structures with face-sharing octahedra close to the NiAs structure type and (3) structures containing fragments of PbI_2 layers with edge-sharing octahedra.

The structures of the first two groups have distorted close-packed layers of anions and organic cations (Figure 1), if we consider the centers of mass of organic cations taken as spheres, where each ion has six nearest neighbors in close-packed layers.

The first group of solvates close in structure to NaCl is characterized by corner-sharing octahedra and includes $(FA)_2PbBr_4·DMSO$, $(MA)_8Pb_{18}I_{44}·x\,GBL$, $(MA)_{8-z}Pb_{18-\delta/2}I_{44-\delta-z}·y\,GBL$ and PbI_2-deficient solvates $(MA)_3PbI_5·DMF$ and $(MA)_3PbI_5·DMSO$. Distorted cubic close-packed layers of iodide ions, organic cations and solvent molecules are observed in these structures, while lead ions partially occupy octahedral voids. The $(FA)_2PbBr_4·DMSO$ phase is a subtraction phase of the NaCl structure type, in which

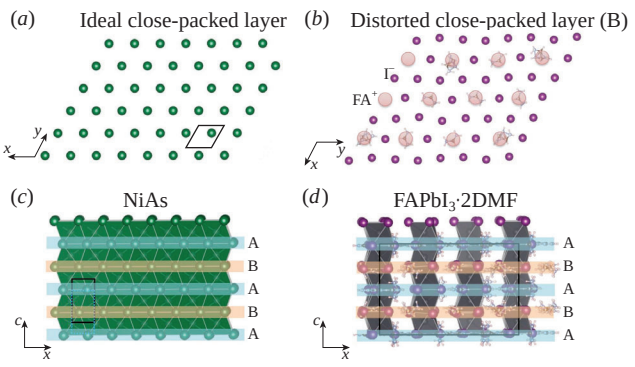

Figure 1 (*a*),(*c*) NiAs structure with ideal hexagonal close-packed layers and (*b*),(*d*) $FAPbI_3·2DMF$ structure with distorted hexagonal close-packed layers formed by anions and organic cations.

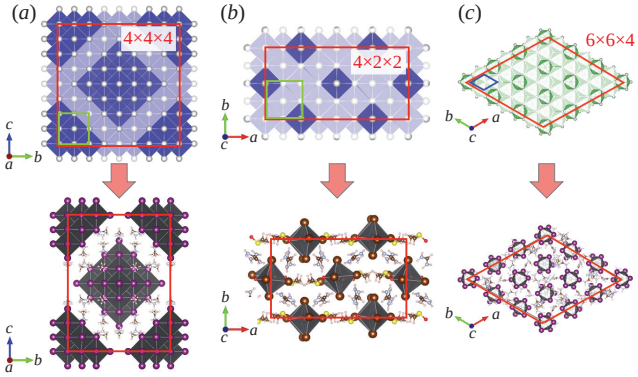

Figure 2 Relationships of solvate structures with their structural prototypes: (*a*) $(MA)_8Pb_{18}I_{44}·x\,GBL$ with NaCl, (*b*) $(FA)_2PbBr_4·DMSO$ with NaCl and (*c*) $(FA)_5Pb_2I_9·0.5DMSO$ with NiAs.

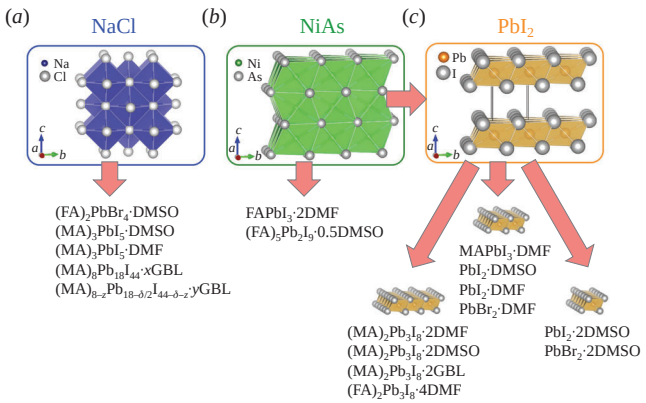

Figure 3 The relationship between the structure of solvates formed in the MAX–PbX_2–Solv and FAX–PbX_2–Solv systems (X = I, Br; Solv = DMSO, DMF, GBL) and the structure types of NaCl, NiAs and PbI_2.

formamidinium cations, Br^- anions and DMSO molecules form a distorted three-layer closest packing, where DMSO molecules occupy two adjacent cuboctahedral sites, and Pb^{2+} ions occupy 1/6 of the octahedral voids [Figure 2(*b*)]. The $(MA)_8Pb_{18}I_{44}·x$GBL and $(MA)_{8-z}Pb_{18-\delta/2}I_{44-\delta-z}·y$GBL solvates consist of $[Pb_{18}I_{44}]^{8-}$ clusters with motifs resembling the NaCl structure. In these structures, the PbI_6 octahedra are connected along edges and vertices, which corresponds to the NaCl structure type [Figure 2(*a*)]. Furthermore, the structure of NaCl can also be considered as a structural analogue for phases consisting of chains of corner-sharing octahedra, such as $(MA)_3PbI_5·$DMF and $(MA)_3PbI_5·$DMSO, although they lack close-packed layers due to large chain distortions and their non-translational shift relative to each other.

The second group of solvates resembling the structure of NiAs includes the $(FA)_5Pb_2I_9·0.5$DMSO and $FAPbI_3·2$DMF phases, which consist of face-sharing octahedra forming dimers and chains with distorted hexagonal closest packings, respectively. The crystal structure of $(FA)_5Pb_2I_9·0.5$DMSO can be considered as a subtraction phase with respect to the NiAs structure with a $6 \times 6 \times 4$ supercell, where Pb^{2+} ions occupy 1/8 of the octahedral voids. Close-packing layers in this structure are formed by FA^+ cations, I^- anions and DMSO molecules [Figure 2(*c*)]. In this case, the sites occupied by DMSO molecules have a partial population, and as a result, DMSO molecules occupy two cuboctahedral sites per formula unit. The crystal structure of the $FAPbI_3·2$DMF phase is represented by isolated ribbons of face-sharing PbI_6 octahedra. Compared to the NiAs structure, the chains in this triclinic structure are shifted relative to each other, which leads to a violation of the symmetry of close-packed layers.

The largest group consists of crystal solvates with structural fragments resembling the PbI_2 phase, which, in turn, is a subtraction phase from NiAs with lead ions layer-by-layer filling half of the octahedral voids. In particular, this group includes $(MA)_2Pb_3I_8·2$DMF, $(MA)_2Pb_3I_8·2$DMSO, $(MA)_2Pb_3I_8·2$GBL and $(FA)_2Pb_3I_8·4$DMF crystal solvates containing $\{Pb_3I_8^{2-}\}_n$ structural motifs, which are ribbons made up of edge-connected triple octahedra. Being differently oriented relative to each other, they form fragments of PbI_2 structural blocks. For example, in the structures of $(MA)_2Pb_3I_8·2$DMF, $(MA)_2Pb_3I_8·2$DMSO, $(MA)_2Pb_3I_8·2$GBL and $(FA)_2Pb_3I_8·4$DMF, the $\{Pb_3I_8^{2-}\}_n$ ribbons are arranged relative to each other in accordance with the presence of different symmetry elements, including additional translational components (grazing reflection planes and helical axes), inversion centers and second-order axes, which is reflected in the symmetry groups of these structures. Finally, this group of solvates includes $MAPbI_3·$DMF, as well as all crystal solvates of lead halides: $PbI_2·$DMSO, $PbI_2·$DMF, $PbBr_2·$DMF, $PbI_2·2$DMSO and $PbBr_2·2$DMSO. These structures also contain ribbons of edge-connected octahedra oriented relative to each other in accordance with the presence of grazing reflection planes, helical axes and inversion centers. A generalized scheme of the relationship between the structure of the solvates formed in the MAX–PbX_2–Solv and FAX–PbX_2–Solv systems (X = I, Br; Solv = DMSO, DMF, GBL) is shown in Figure 3.

From a practical point of view, it is also interesting to consider the hydrates of hybrid perovskites, since water is one of the main factors of perovskite degradation. In this respect, two hydrate phases are known: $MAPbI_3·H_2O$[25] and $(MA)_4PbI_6·2H_2O$.[33] The structure of the former consists of Pb_2I_6 ribbons, as in $MAPbI_3·$DMF, which leads to a reconstruction of the perovskite structure upon its dehydration similar to that observed upon the decomposition of $MAPbI_3·$DMF. In contrast, the dihydrate phase consists of isolated PbI_6 octahedra. Although three hydrate phases of $FAPbI_3$ have been reported recently,[34] their composition has not yet been confirmed by single crystal X-ray diffraction analysis. While lead iodide hydrates have not been reported, there is a $3PbBr_2·2H_2O$ phase[32] consisting of an inorganic framework of bromide anions and eight-coordinated Pb^{2+} cations forming channels in which water molecules are located and every second molecule is connected with lead atoms. Though the compound '$HPbI_3$' has been previously reported, two hydrates have recently been shown to exist instead: $(H_3O)_2Pb_3I_8·6H_2O$ and $H_{0.43}Pb_{0.78}I_2·2H_2O$.[35]

To sum up, the $(FA)_2PbBr_4·$DMSO, $(MA)_8Pb_{18}I_{44}·x$GBL, $(MA)_{8-z}Pb_{18-\delta/2}I_{44-\delta-z}·y$GBL, $(MA)_3PbI_5·$DMF and $(MA)_3PbI_5·$DMSO phases can be considered as phases resembling NaCl with distorted close packing, the $FAPbI_3·2$DMF and $(FA)_5Pb_2I_9·0.5$DMSO phases have structures close to the structure of NiAs with distorted close packing, while the other considered phases [$(MA)_2Pb_3I_8·2$DMF, $(MA)_2Pb_3I_8·2$DMSO, $(MA)_2Pb_3I_8·2$GBL, $(FA)_2Pb_3I_8·4$DMF, $MAPbI_3·$DMF, $PbI_2·$DMSO, $PbI_2·$DMF, $PbBr_2·$DMF, $PbI_2·2$DMSO and $PbBr_2·2$DMSO] consist of differently oriented fragments of the PbI_2 structure.

We believe that the proposed classification, based either on chemical composition or structural similarity, would be useful in the context of the discovered phenomenon of structurally determined inheritance of the morphology of crystal solvate films by light-absorbing perovskite layers prepared by widely used solution techniques. In this regard, the crystal chemical features of crystal solvates as intermediate phases through which hybrid perovskites are formed may turn out to be important when planning approaches to the creation of solar cells with desired functional characteristics.

The work was supported by the Russian Science Foundation (grant no. 19-73-30022).

References

1 W. Li, Z. Wang, F. Deschler, S. Gao, R. H. Friend and A. K. Cheetham, *Nat. Rev. Mater.*, 2017, **2**, 16099.
2 J. Huang, Y. Yuan, Y. Shao and Y. Yan, *Nat. Rev. Mater.*, 2017, **2**, 17042.
3 N.-G. Park, M. Grätzel, T. Miyasaka, K. Zhu and K. Emery, *Nat. Energy*, 2016, **1**, 16152.
4 E. A. Eliseev, D. G. Filatova, A. S. Chizhov, M. N. Rumyantseva and A. M. Gaskov, *Mendeleev Commun.*, 2021, **31**, 462.
5 J. Seo, J. H. Noh and S. I. Seok, *Acc. Chem. Res.*, 2016, **49**, 562.
6 A. S. Tutantsev, N. N. Udalova, S. A. Fateev, A. A. Petrov, C. Wang, E. G. Maksimov, E. A. Goodilin and A. B. Tarasov, *J. Phys. Chem. C*, 2020, **124**, 11117.
7 D. V. Amasev, Sh. R. Saitov, V. G. Mikhalevich, A. R. Tameev and A. G. Kazanskii, *Mendeleev Commun.*, 2021, **31**, 469.
8 S. A. Fateev, A. A. Petrov, V. N. Khrustalev, P. V. Dorovatovskii, Y. V. Zubavichus, E. A. Goodilin and A. B. Tarasov, *Chem. Mater.*, 2018, **30**, 5237.
9 N. J. Jeon, J. H. Noh, Y. C. Kim, W. S. Yang, S. Ryu and S. I. Seok, *Nat. Mater.*, 2014, **13**, 897.
10 N. Ahn, D.-Y. Son, I.-H. Jang, S. M. Kang, M. Choi and N.-G. Park, *J. Am. Chem. Soc.*, 2015, **137**, 8696.

11 A. A. Petrov, N. Pellet, J.-Y. Seo, N. A. Belich, D. Yu. Kovalev, A. V. Shevelkov, E. A. Goodilin, S. M. Zakeeruddin, A. B. Tarasov and M. Graetzel, *Chem. Mater.*, 2017, **29**, 587.
12 A. A. Petrov, I. P. Sokolova, N. A. Belich, G. S. Peters, P. V. Dorovatovskii, Y. V. Zubavichus, V. N. Khrustalev, A. V. Petrov, M. Grätzel, E. A. Goodilin and A. B. Tarasov, *J. Phys. Chem. C*, 2017, **121**, 20739.
13 A. A. Petrov, S. A. Fateev, V. N. Khrustalev, Y. Li, P. V. Dorovatovskii, Y. V. Zubavichus, E. A. Goodilin and A. B. Tarasov, *Chem. Mater.*, 2020, **32**, 7739.
14 W. S. Yang, J. H. Noh, N. J. Jeon, Y. C. Kim, S. Ryu, J. Seo and S. I. Seok, *Science*, 2015, **348**, 1234.
15 B. Park, H. W. Kwon, Y. Lee, D. Y. Lee, M. G. Kim, G. Kim, K. Kim, Y. K. Kim, J. Im, T. J. Shin and S. I. Seok, *Nat. Energy*, 2021, **6**, 419.
16 Y. Jo, K. S. Oh, M. Kim, K.-H. Kim, H. Lee, C.-W. Lee and D. S. Kim, *Adv. Mater. Interfaces*, 2016, **3**, 1500768.
17 S. A. Adonin, M. N. Sokolov, M. E. Rakhmanova, A. I. Smolentsev, I. V. Korolkov, S. G. Kozlova and V. P. Fedin, *Inorg. Chem. Commun.*, 2015, **54**, 89.
18 S. A. Adonin, M. E. Rakhmanova, A. I. Smolentsev, I. V. Korolkov, M. N. Sokolov and V. P. Fedin, *New J. Chem.*, 2015, **39**, 5529.
19 S. A. Adonin, M. N. Sokolov and V. P. Fedin, *Russ. J. Inorg. Chem.*, 2017, **62**, 1789.
20 N. Mercier, N. Louvain and W. Bi, *CrystEngComm*, 2009, **11**, 720.
21 S. A. Adonin, M. N. Sokolov and V. P. Fedin, *Coord. Chem. Rev.*, 2016, **312**, 1.
22 L.-M. Wu, X.-T. Wu and L. Chen, *Coord. Chem. Rev.*, 2009, **253**, 2787.
23 J. Cao, X. Jing, J. Yan, C. Hu, R. Chen, J. Yin, J. Li and N. Zheng, *J. Am. Chem. Soc.*, 2016, **138**, 9919.
24 Y. Rong, Z. Tang, Y. Zhao, X. Zhong, S. Venkatesan, H. Graham, M. Patton, Y. Jing, A. M. Guloy and Y. Yao, *Nanoscale*, 2015, **7**, 10595.
25 F. Hao, C. C. Stoumpos, Z. Liu, R. P. H. Chang and M. G. Kanatzidis, *J. Am. Chem. Soc.*, 2014, **136**, 16411.
26 M. Ozaki, A. Shimazaki, M. Jung, Y. Nakaike, N. Maruyama, S. Yakumaru, A. I. Rafieh, T. Sasamori, N. Tokitoh, P. Ekanayake, Y. Murata, R. Murdey and A. Wakamiya, *Angew. Chem., Int. Ed.*, 2019, **58**, 9389.
27 W. Mao, J. Zheng, Y. Zhang, A. S. R. Chesman, Q. Ou, J. Hicks, F. Li, Z. Wang, B. Graystone, T. D. M. Bell, M. Uller Rothmann, N. W. Duffy, L. Spiccia, Y.-B. Cheng, Q. Bao and U. Bach, *Angew. Chem.*, 2017, **129**, 12660.
28 C. Hu, S. B. Shivarudraiah, H. H. Y. Sung, I. D. Williams, J. E. Halpert and S. Yang, *Sol. RRL*, 2021, **5**, 2000712.
29 M. Ozaki, Y. Ishikura, M. A. Truong, J. Liu, I. Okada, T. Tanabe, S. Sekimoto, T. Ohtsuki, Y. Murata, R. Murdey and A. Wakamiya, *J. Mater. Chem. A*, 2019, **7**, 16947.
30 I. Wharf, T. Gramstad, R. Makhija and M. Onyszchuk, *Can. J. Chem.*, 1976, **54**, 3430.
31 A. Wakamiya, M. Endo, T. Sasamori, N. Tokitoh, Y. Ogomi, S. Hayase and Y. Murata, *Chem. Lett.*, 2014, **43**, 711.
32 M. Liu, J. Zhao, Z. Luo, Z. Sun, N. Pan, H. Ding and X. Wang, *Chem. Mater.*, 2018, **30**, 5846.
33 B. R. Vincent, K. N. Robertson, T. S. Cameron and O. Knop, *Can. J. Chem.*, 1987, **65**, 1042.
34 R. T. Wang, A. F. Xu, W. Li, Y. Li and G. Xu, *J. Phys. Chem. Lett.*, 2021, **12**, 5332.
35 M. Daub and H. Hillebrecht, *Z. Anorg. Allg. Chem.*, 2018, **644**, 1393.

Received: 1st December 2021; Com. 21/6766